Electronic Supplementary Information

Pyrrolopyrrole aza boron dipyrromethene based two-photon fluorescent probes for subcellular imaging

Yimin Zhou, Chao Ma, Nengyue Gao, Qiong Wang, Pui-Chi Lo,* Kam Sing Wong, Qing-Hua Xu, Takumi Kinoshita and Dennis K. P. Ng*

Contents

Fig. S1 Electronic absorption spectra of **17** at various concentrations in deionised water (with 0.3% v/v Tween 80 and 1% v/v DMF). The inset plots the Q-band absorbance versus the concentration of **17.**

Fig. S2 Electronic absorption spectra of **18** at various concentrations in deionised water (with 0.3% v/v Tween 80 and 1% v/v DMF). The inset plots the Q-band absorbance versus the concentration of **18.**

Fig. S3 Electronic absorption spectra of **19** at various concentrations in deionised water (with 0.3% v/v Tween 80 and 1% v/v DMF). The inset plots the Q-band absorbance versus the concentration of **19.**

Fig. S4 Simulation of the TPA cross-sections of the model compound for **19** with reduced chain length using the ADF programme on the PBE/DZ basis condition.

Fig. S5 Simulation of the one-photon absorption spectrum of the model compound for **19** with reduced chain length using a time-dependent DFT method.

Fig. S6 ^{1}H NMR spectrum of **1** in $CDCl_3$.

Fig. S7 $^{13}C\{^{1}H\}$ NMR spectrum of **1** in $CDCl_3$.

Fig. S8 ^{1}H NMR spectrum of **7** in $CDCl_3$.

Fig. S9 $^{13}C\{^{1}H\}$ NMR spectrum of **7** in $CDCl_3$.

Fig. S10 ^{1}H NMR spectrum of **8** in $CDCl_3$.

Fig. S11 $^{13}C\{^{1}H\}$ NMR spectrum of **8** in $CDCl_3$.

Fig. S12 ^{1}H NMR spectrum of **9** in $CDCl_3$.

Fig. S13 ^{1}H NMR spectrum of **10** in $CDCl_3$.

Fig. S14 ^{1}H NMR spectrum of **12** in $CDCl_3$.

Fig. S15 ^{1}H NMR spectrum of **13** in $CDCl_3$.

Fig. S16 ^{1}H NMR spectrum of **17** in $CDCl_3$.

Fig. S17 ^{1}H NMR spectrum of **18** in $CDCl_3$.

Fig. S18 ^{1}H NMR spectrum of **19** in $CDCl_3$.

Fig. S19 ESI mass spectrum of **1**.

Fig. S20 ESI mass spectrum of **7**.

Fig. S21 ESI mass spectrum of **8**.

Fig. S22 MALDI-TOF mass spectrum of **9**. The inset shows the enlarged isotopic envelop of the molecular ion peak.

Fig. S23 MALDI-TOF mass spectrum of **10**. The inset shows the enlarged isotopic envelop of the molecular ion peak.

Fig. S24 ESI mass spectrum of **12**. The inset shows the enlarged isotopic envelop of the molecular ion peak.

Fig. S25 ESI mass spectrum of **13**. The inset shows the enlarged isotopic envelop of the molecular ion peak.

Fig. S26 ESI mass spectrum of **17**. The inset shows the enlarged isotopic envelop of the molecular ion peak.

Fig. S27 ESI mass spectrum of **18**. The inset shows the enlarged isotopic envelop of the molecular ion peak.

Fig. S28 ESI mass spectrum of **19**. The inset shows the enlarged isotopic envelop of the molecular ion peak.

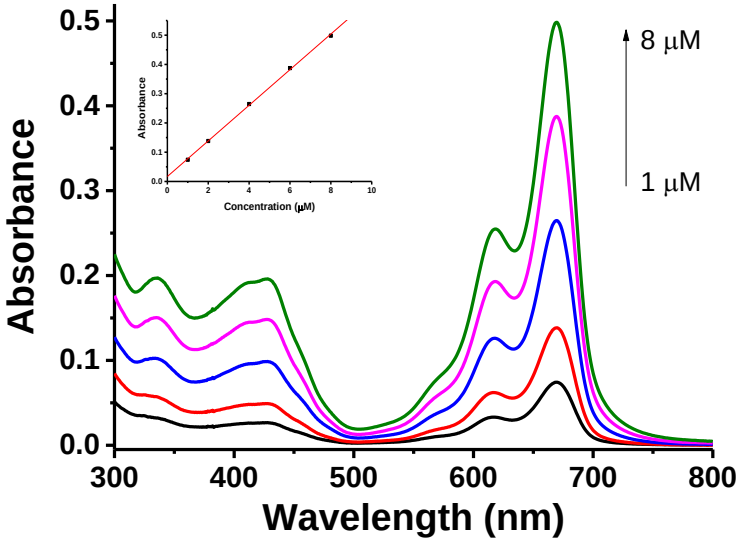

Fig. S1 Electronic absorption spectra of **17** at various concentrations in deionised water (with 0.3% v/v Tween 80 and 1% v/v DMF). The inset plots the Q-band absorbance versus the concentration of **17.**

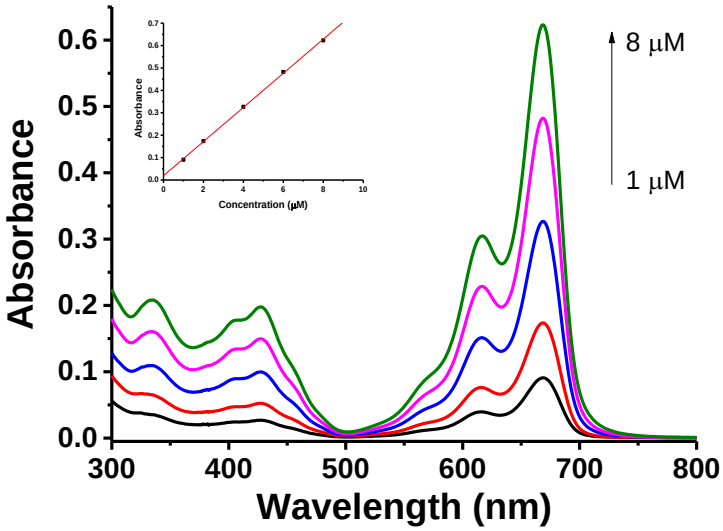

Fig. S2 Electronic absorption spectra of **18** at various concentrations in deionised water (with 0.3% v/v Tween 80 and 1% v/v DMF). The inset plots the Q-band absorbance versus the concentration of **18.**

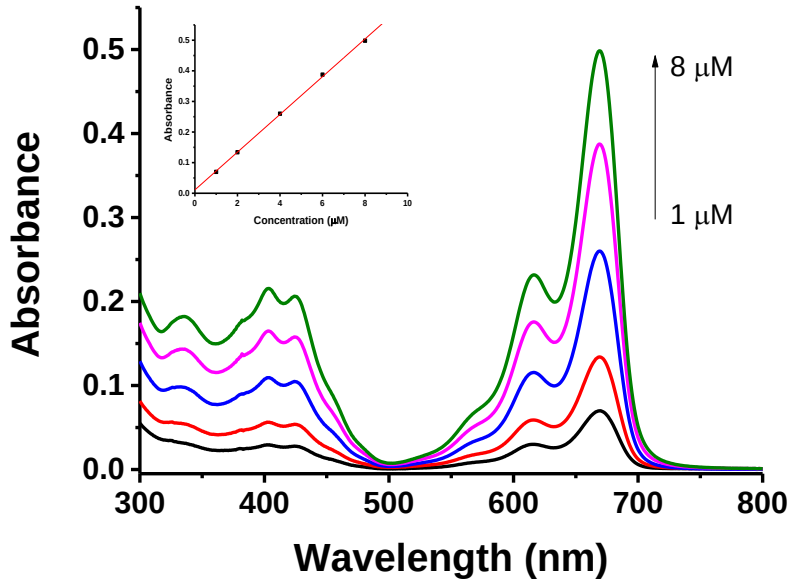

Fig. S3 Electronic absorption spectra of **19** at various concentrations in deionised water (with 0.3% v/v Tween 80 and 1% v/v DMF). The inset plots the Q-band absorbance versus the concentration of **19.**

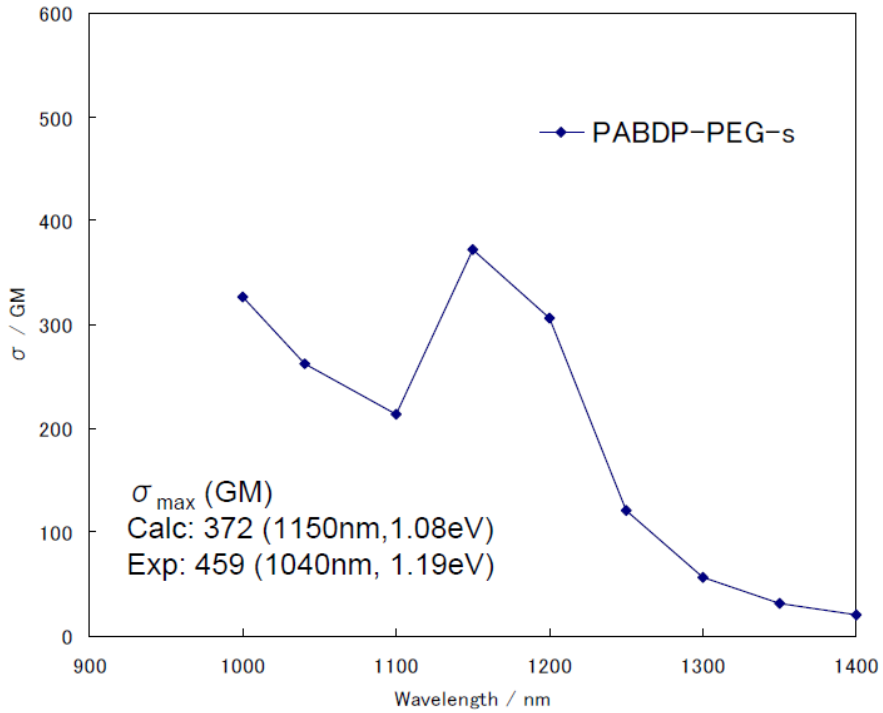

Fig. S4 Simulation of the TPA cross-sections of the model compound for **19** with reduced chain length using the ADF programme on the PBE/DZ basis condition.

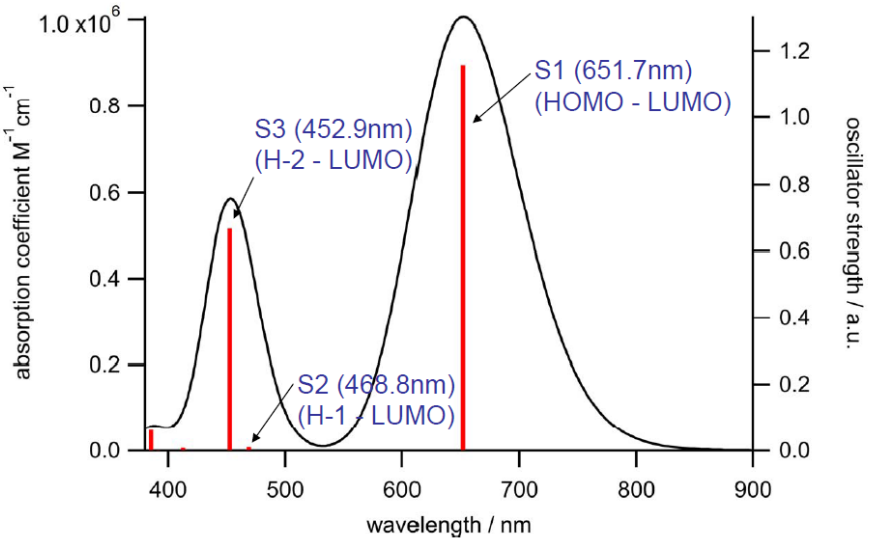

Fig. S5 Simulation of the one-photon absorption spectrum of the model compound for **19** with reduced chain length using a time-dependent DFT method.

In all the following ^{1}H and $^{13}C\{^{1}H\}$ NMR spectra, residual solvent (or solvent) signals are marked with asterisks.

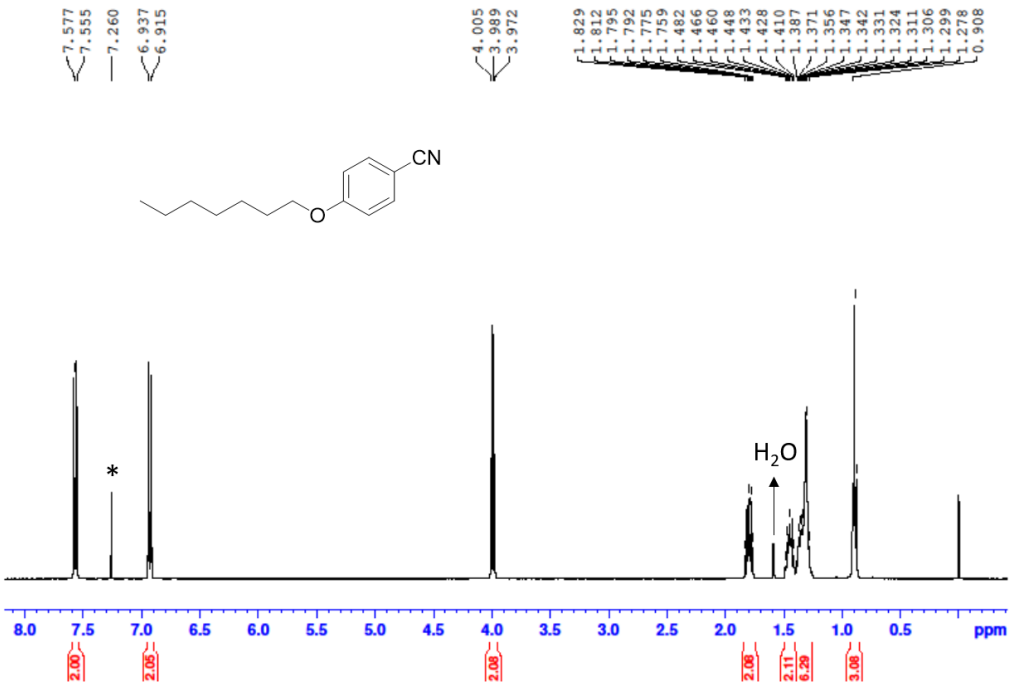

Fig. S6 ^{1}H NMR spectrum of **1** in $CDCl_3$.

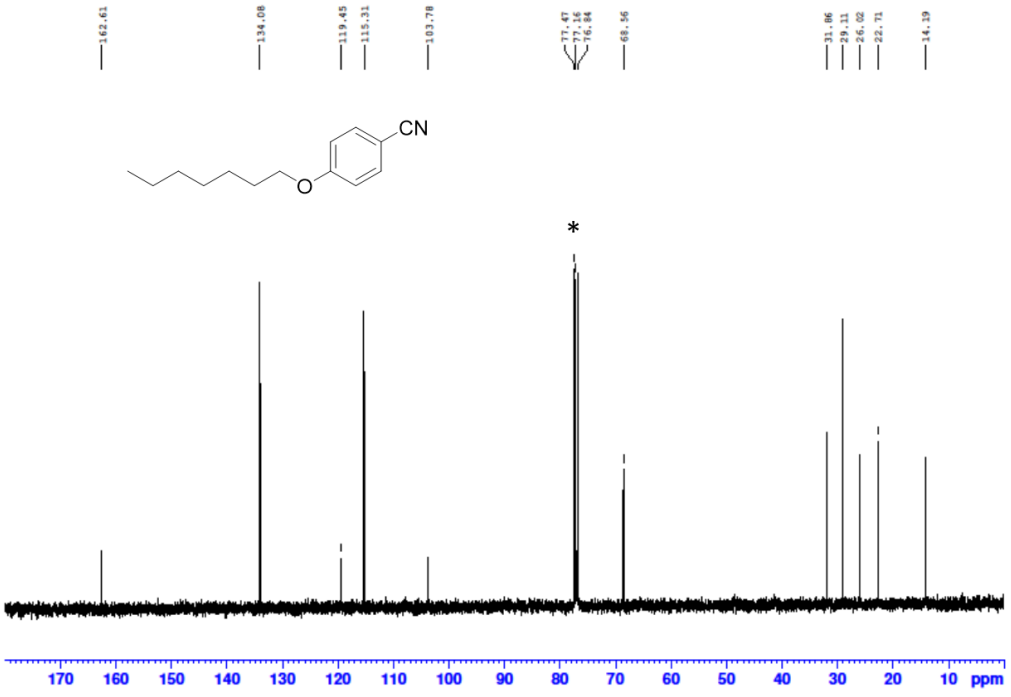

Fig. S7 $^{13}C\{^{1}H\}$ NMR spectrum of **1** in $CDCl_3$.

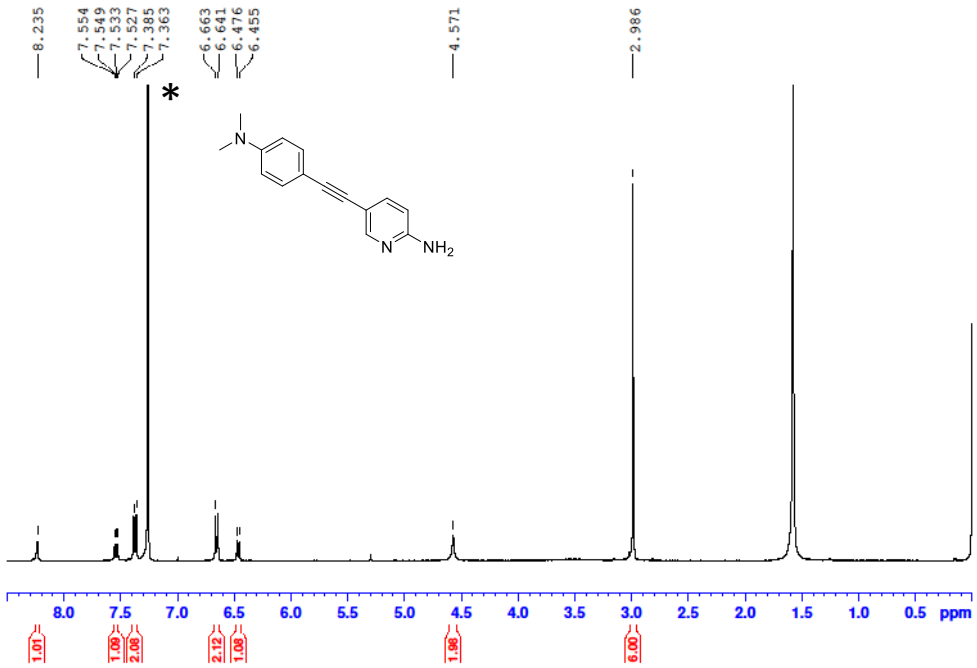

Fig. S8 ^{1}H NMR spectrum of **7** in $CDCl_3$.

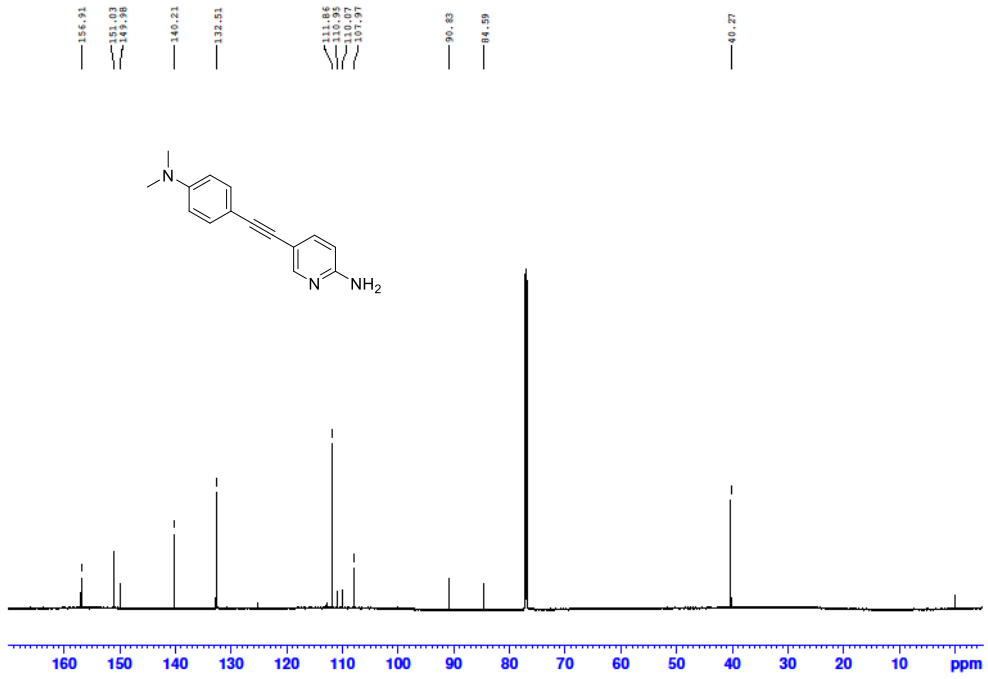

Fig. S9 $^{13}C\{^{1}H\}$ NMR spectrum of **7** in $CDCl_3$.

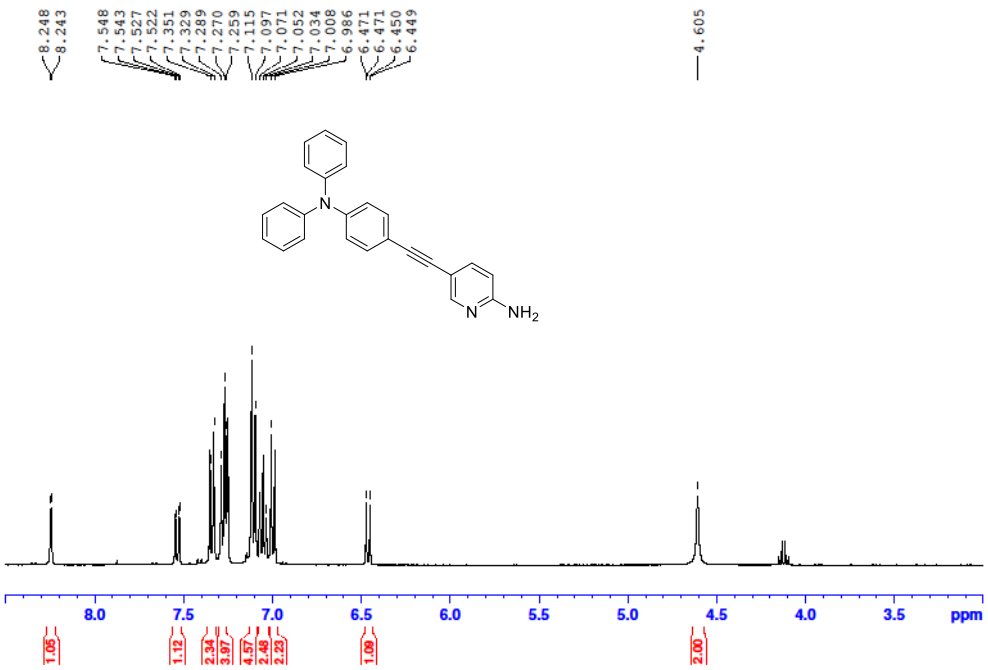

Fig. S10 ^{1}H NMR spectrum of **8** in $CDCl_3$.

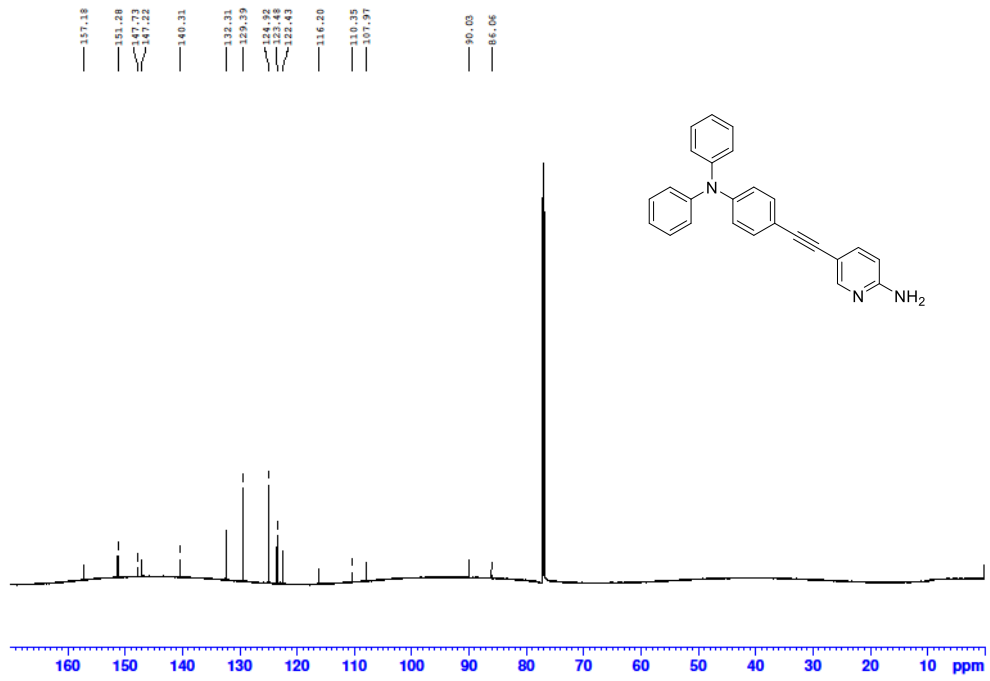

Fig. S11 $^{13}C\{^{1}H\}$ NMR spectrum of **8** in $CDCl_3$.

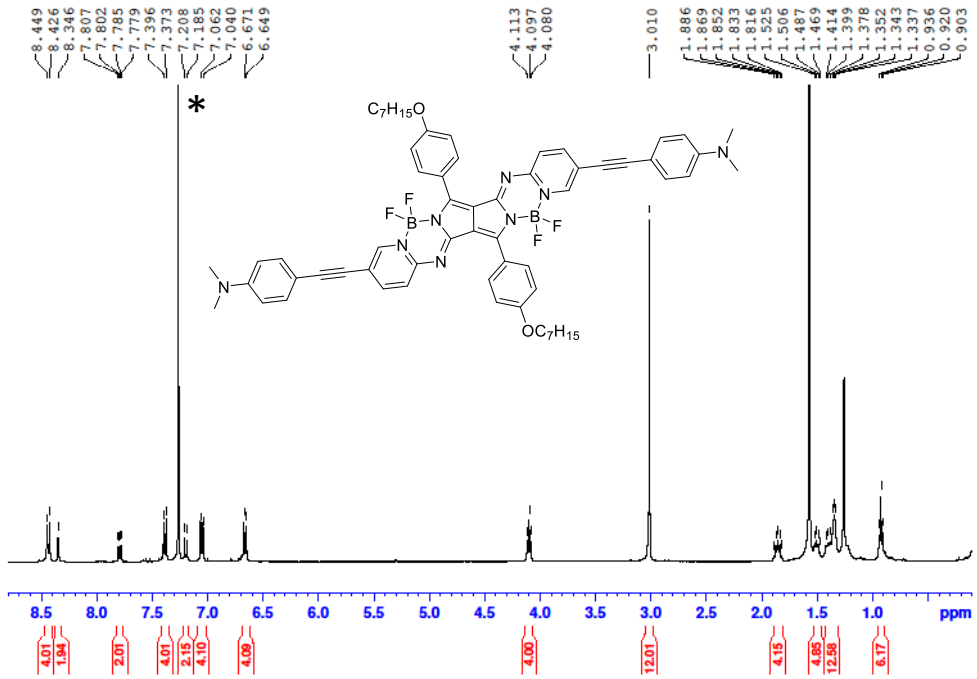

Fig. S12 ^{1}H NMR spectrum of **9** in $CDCl_3$.

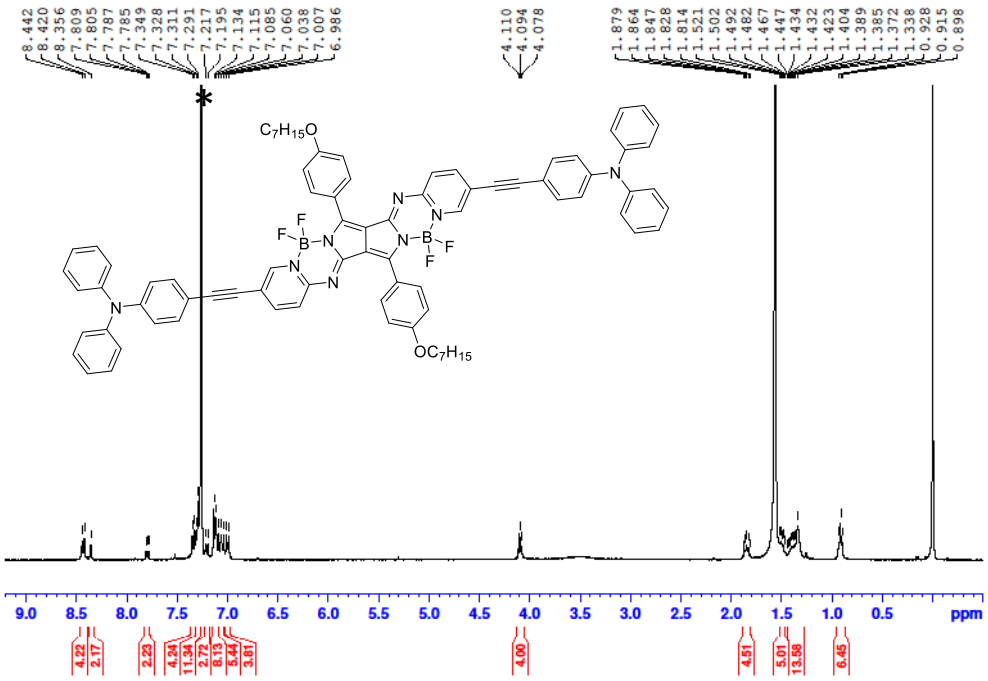

Fig. S13 ^{1}H NMR spectrum of **10** in $CDCl_3$.

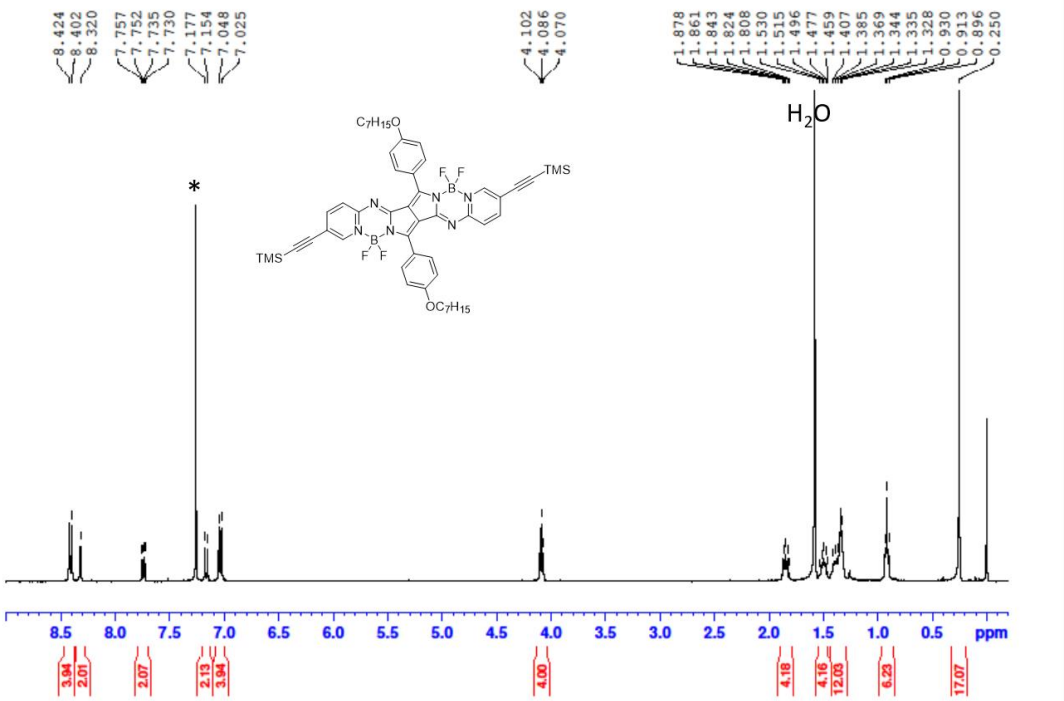

Fig. S14 ^{1}H NMR spectrum of **12** in $CDCl_3$.

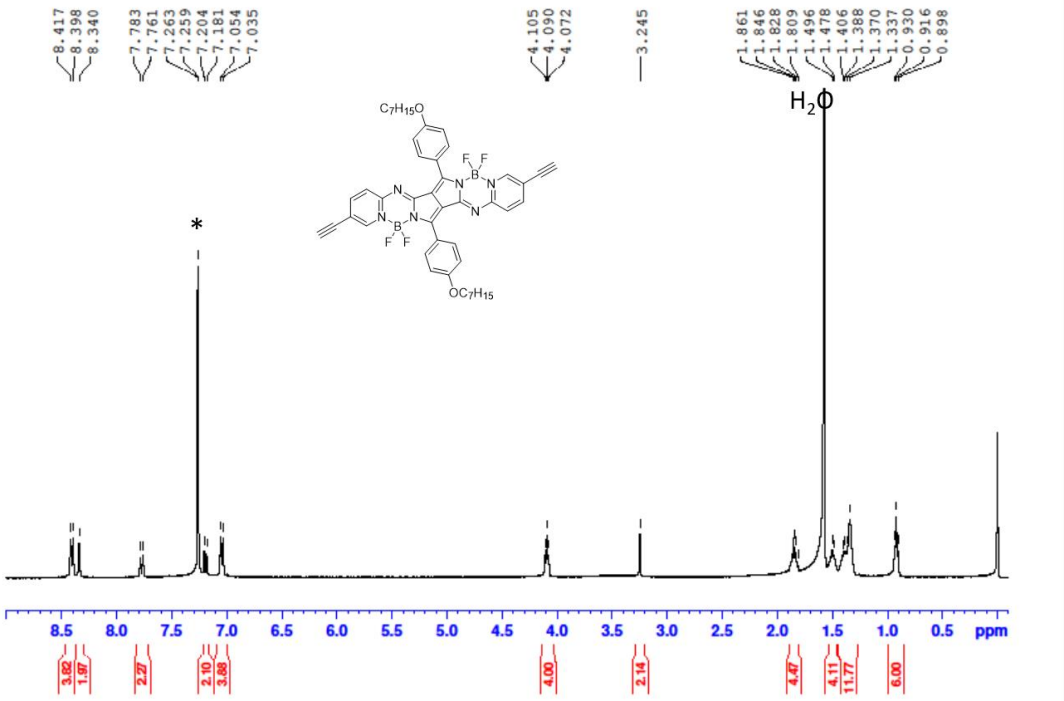

Fig. S15 ^{1}H NMR spectrum of **13** in $CDCl_3$.

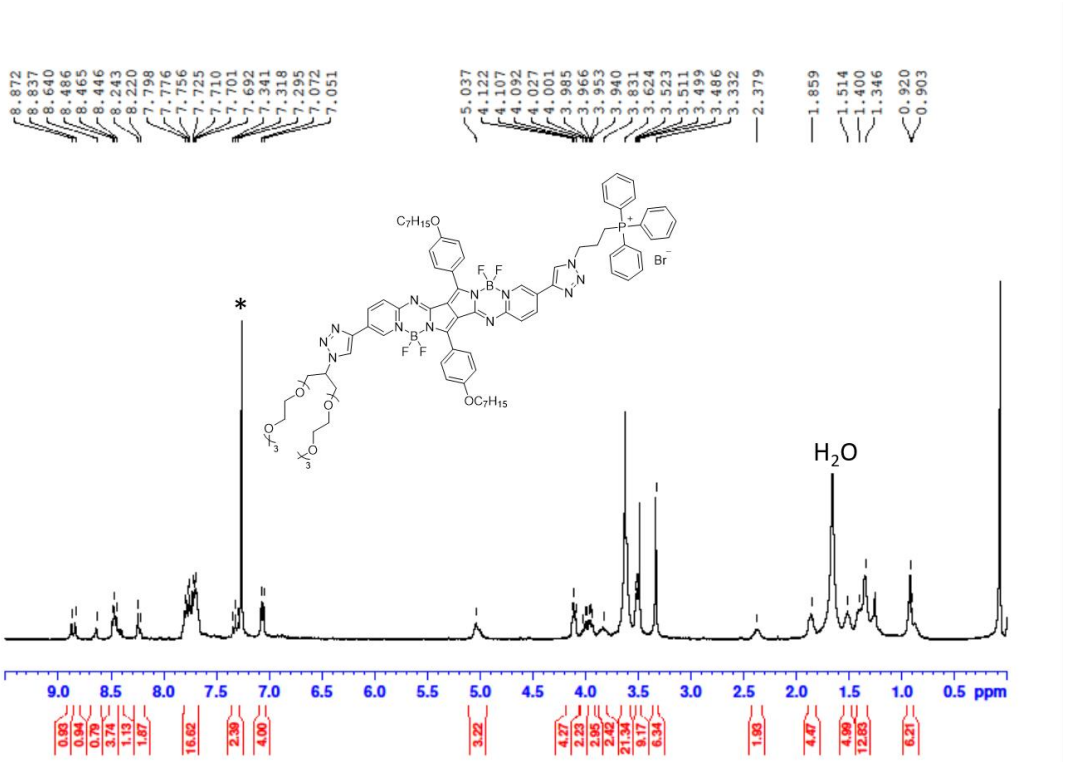

Fig. S16 ^{1}H NMR spectrum of **17** in $CDCl_3$.

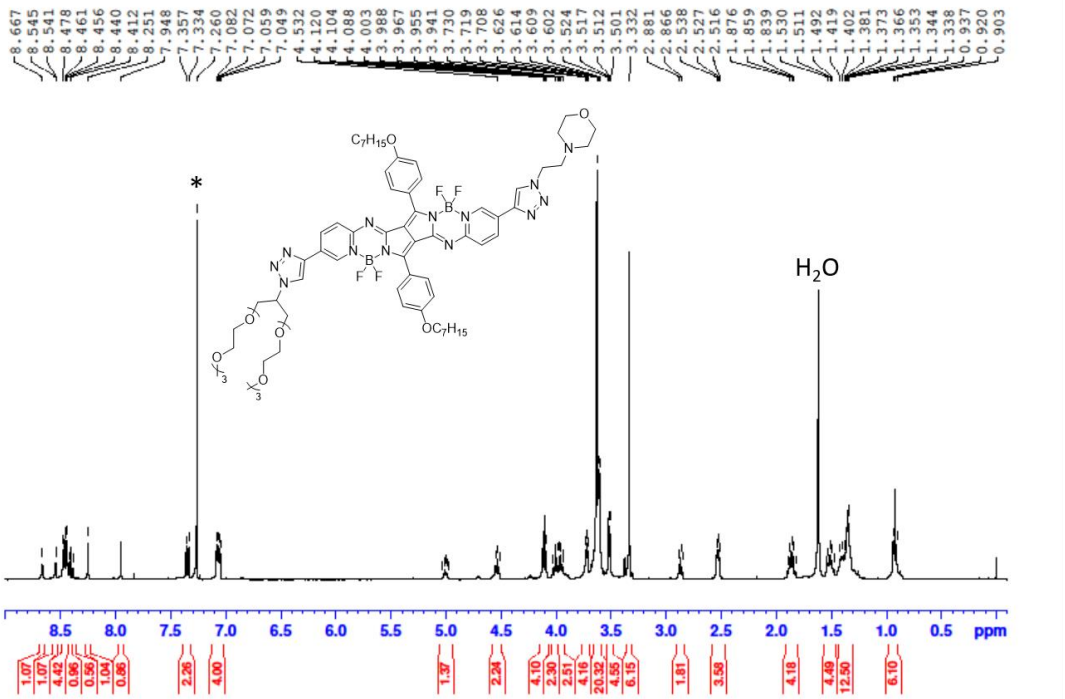

Fig. S17 ^{1}H NMR spectrum of **18** in $CDCl_3$.

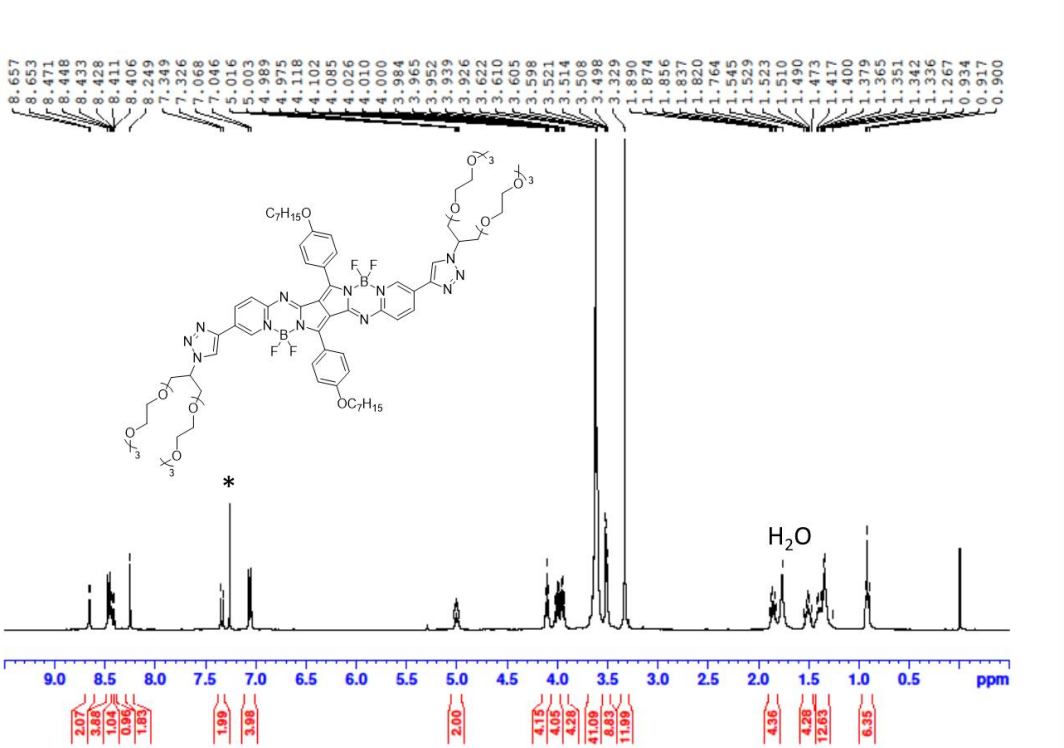

Fig. S18 ^{1}H NMR spectrum of **19** in $CDCl_3$.

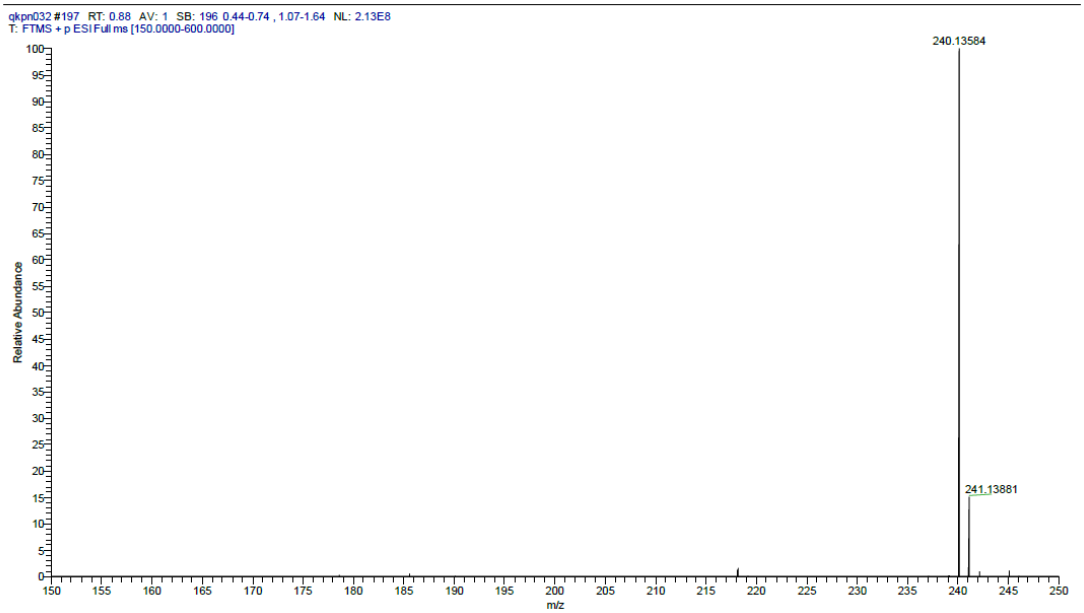

Fig. S19 ESI mass spectrum of **1**.

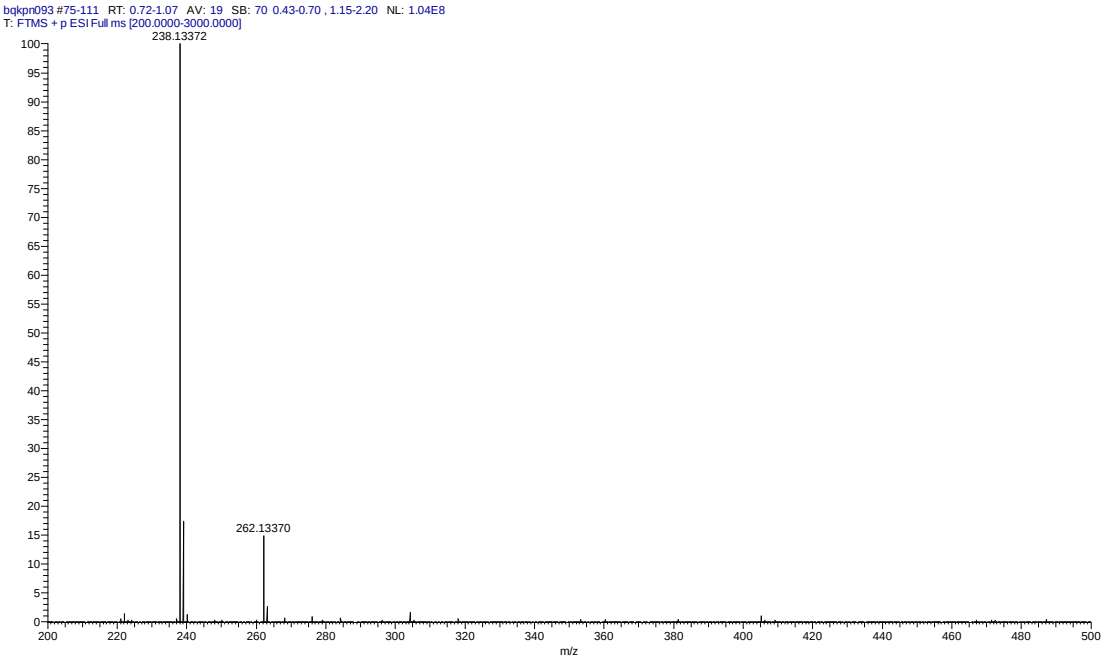

Fig. S20 ESI mass spectrum of **7**.

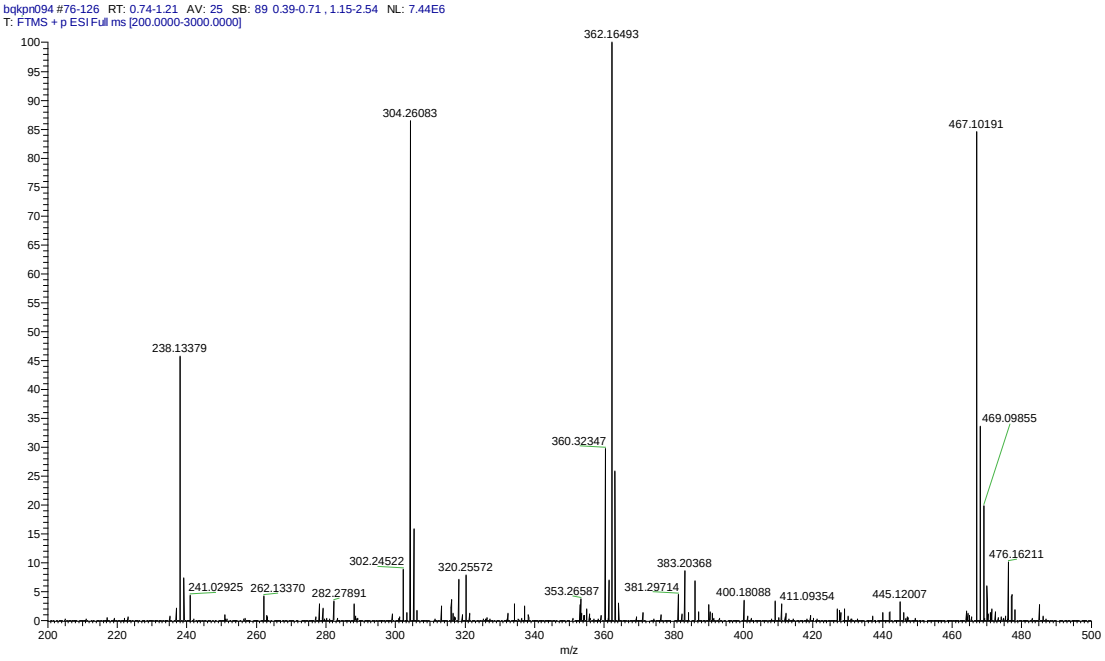

Fig. S21 ESI mass spectrum of **8**.

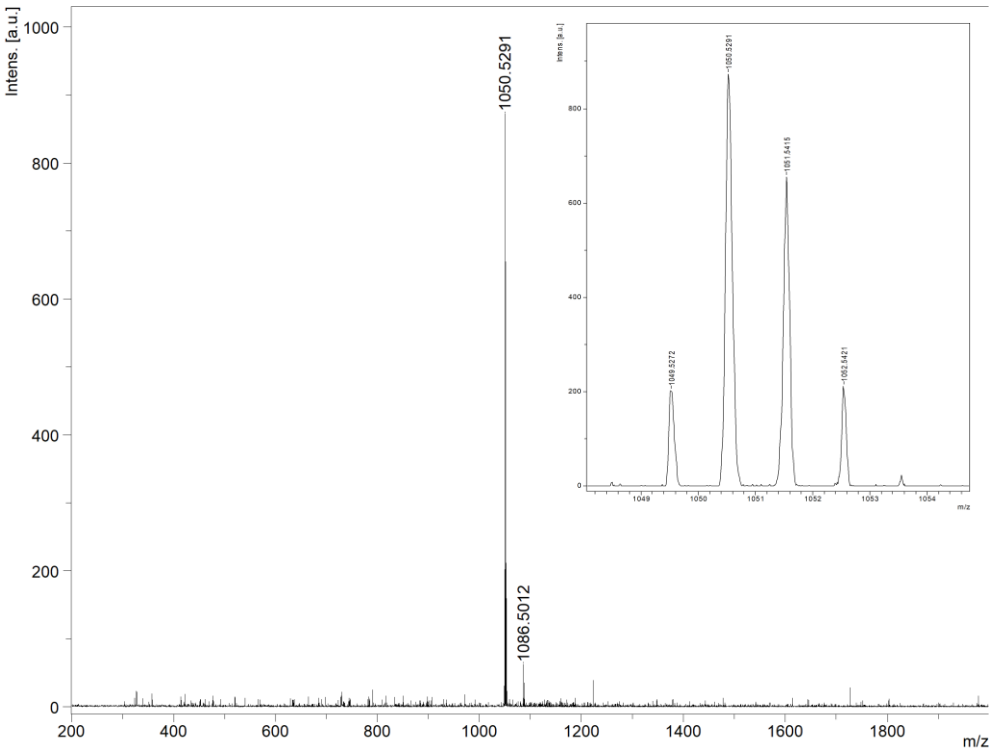

Fig. S22 MALDI-TOF mass spectrum of **9**. The inset shows the enlarged isotopic envelop of the molecular ion peak.

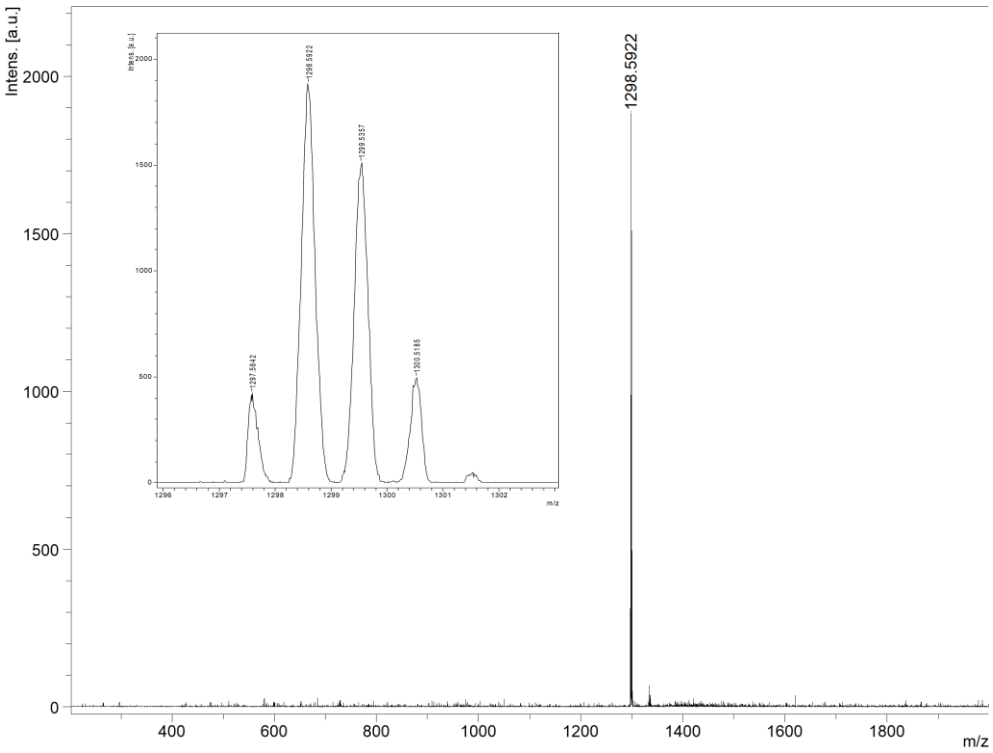

Fig. S23 MALDI-TOF mass spectrum of **10**. The inset shows the enlarged isotopic envelop of the molecular ion peak.

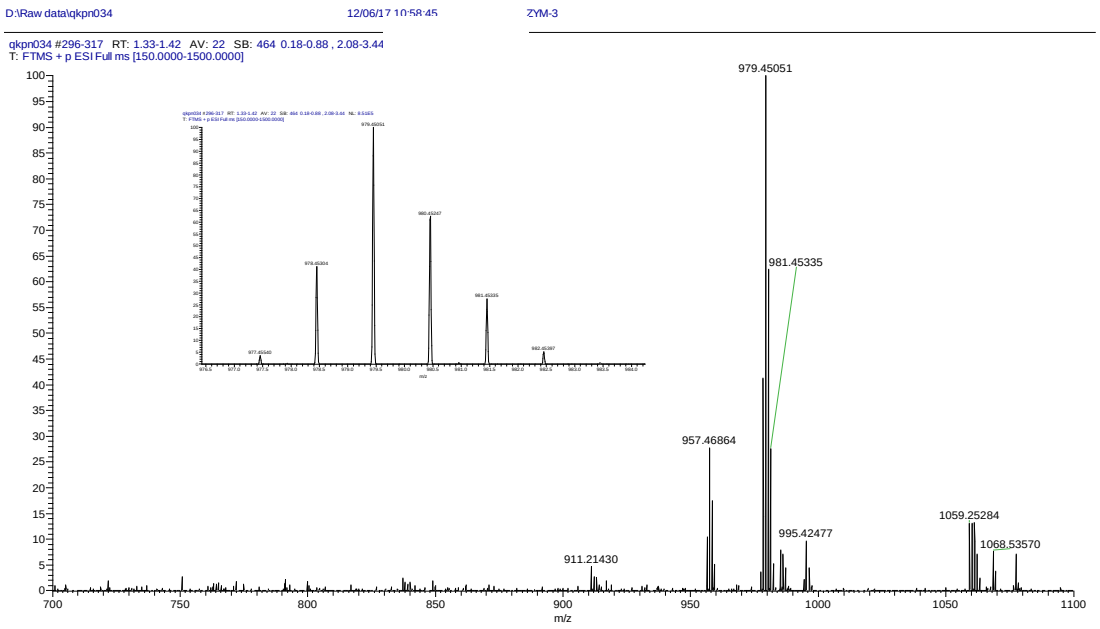

Fig. S24 ESI mass spectrum of **12**. The inset shows the enlarged isotopic envelop of the molecular ion peak.

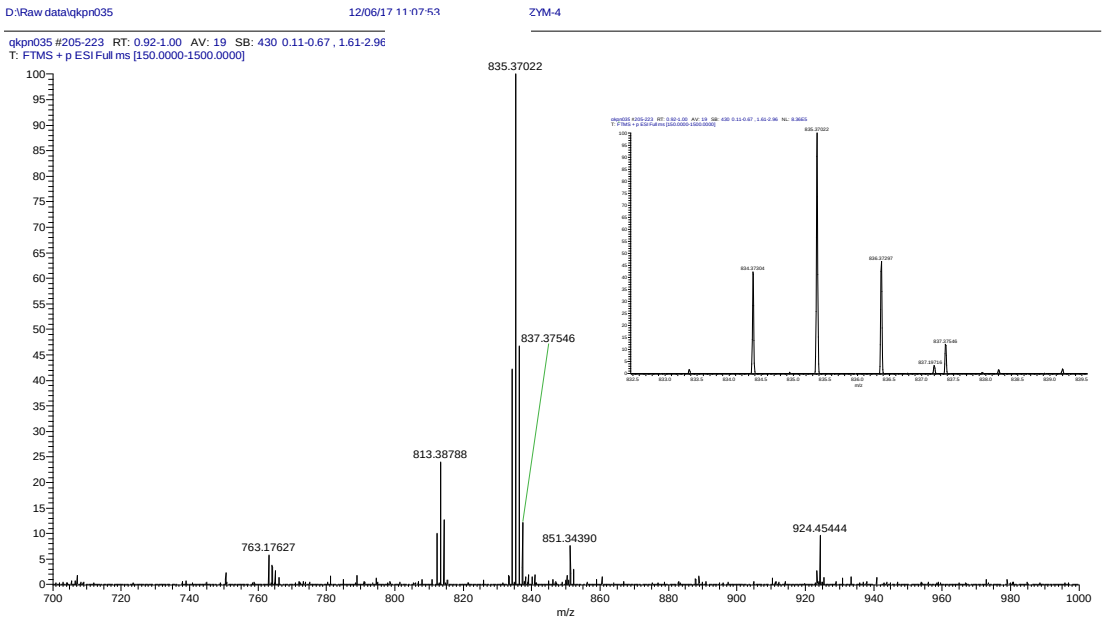

Fig. S25 ESI mass spectrum of **13**. The inset shows the enlarged isotopic envelop of the molecular ion peak.

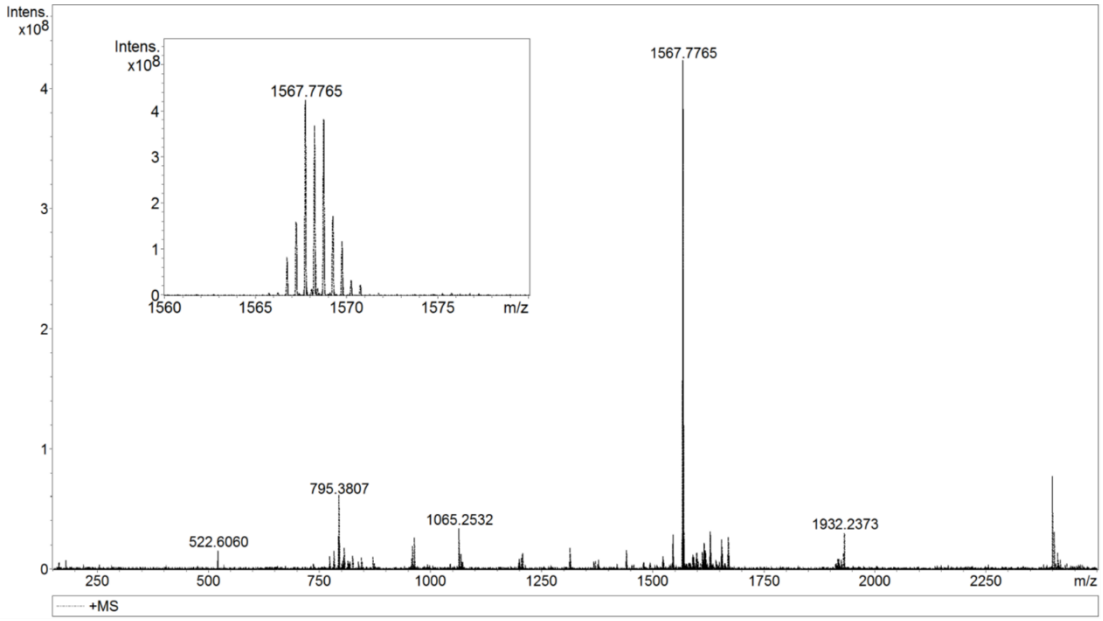

Fig. S26 ESI mass spectrum of **17**. The inset shows the enlarged isotopic envelop of the molecular ion peak.

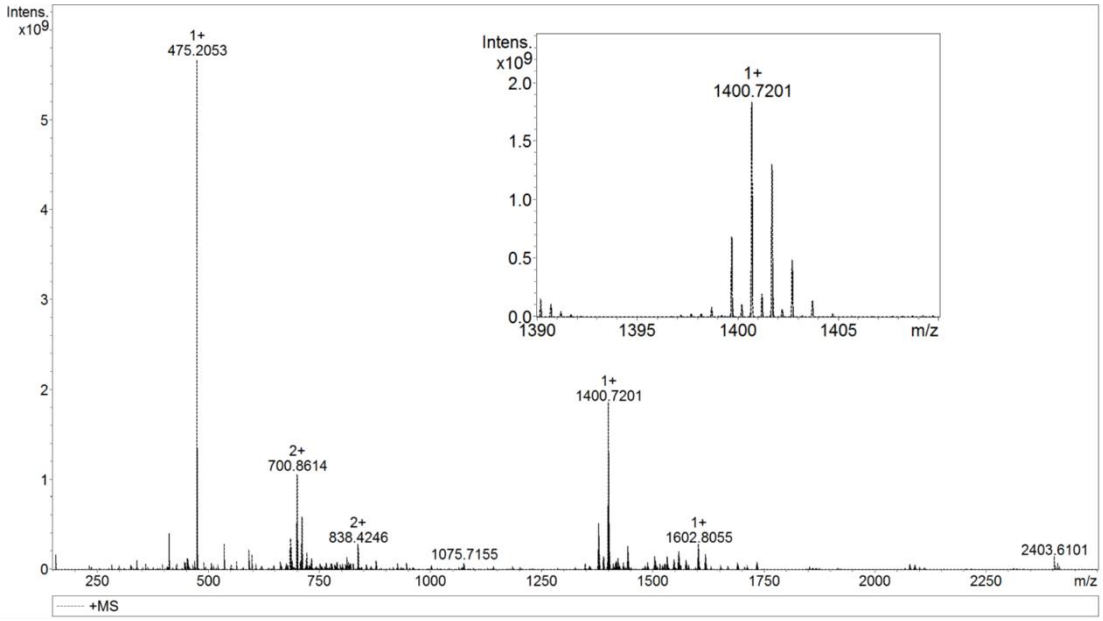

Fig. S27 ESI mass spectrum of **18**. The inset shows the enlarged isotopic envelop of the molecular ion peak.

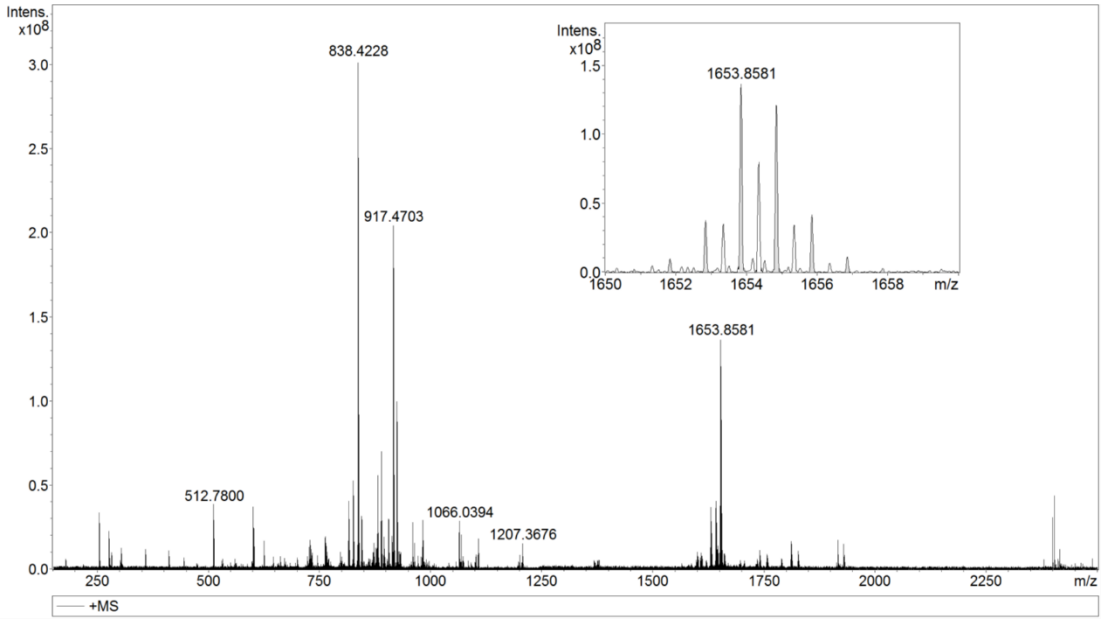

Fig. S28 ESI mass spectrum of **19**. The inset shows the enlarged isotopic envelop of the molecular ion peak.